Silylated carbodiimides in molecular and extended structures

Peter Kroll
Department of Chemistry and Chemical Biology, Baker Laboratory, Cornell University, Ithaca, New York 14853-1301

Ralf Riedel
Fachbereich Materialwissenschaft, Fachgebiet Disperse Feststoffe, Technische Universität Darmstadt, Petersenstrasse 23, D-64287 Darmstadt, Germany

Roald Hoffmann
Department of Chemistry and Chemical Biology, Baker Laboratory, Cornell University, Ithaca, New York 14853-1301
(Received 29 October 1998)

This work studies the ternary Si-C-N phases SiC_2N_4 and Si_2CN_4, exploiting an analogy between the NCN and O groups. Starting from the molecular model of *N,N′*-bis(trimethylsilyl)-carbodiimide and proceeding to extended models, we calculate that the energy hypersurface associated with the Si-N=C bond angle φ_N is very shallow, for both molecular and extended structures. We propose a crystal structure for the low-temperature modification α-SiC_2N_4 in space group $P4_322$ (95), which is 40 meV ($\sim$4 kJ/mol) lower in energy than an ideal cubic arrangement in space group $Pn\bar{3}m$. A second structure, β-SiC_2N_4 [space group $P\bar{4}n2$ (118)], is slightly higher in energy than α-SiC_2N_4, but still more stable than the cubic structure, and may be the high-temperature structure of SiC_2N_4. Both variants of SiC_2N_4 show a small bulk modulus of about 8 GPa ($\sim$0.13 Mbar), suggesting a high compressibility of these nonoxide covalently bonded materials. For Si_2CN_4 we refined the crystal structure of the compound within the experimentally determined space group $Aba2$ (41). We also found a second candidate nearly equal in energy, with space group $Cmc2_1$, differing only in the connection pattern of the SiN_2 layered sheets. Both ternary compounds appear to be thermodynamically unstable with respect to decomposition into Si_3N_4, C, and molecular N_2. [S0163-1829(99)02629-6]

INTRODUCTION

Up to now, there appear to be no thermodynamically stable ternary Si-C-N-phases in the ternary phase diagram Si-C-N.[1,2] Besides the elements silicon (Si), carbon (C), and nitrogen (N), only two binary phases, silicon carbide (SiC) and silicon nitride (Si_3N_4), are reported to be thermodynamically stable. From the perspective of a materials scientist, by far the most relevant materials in this system are the elemental phases of silicon and carbon, in their various polymorphs. SiC is more and more important as a material for high-temperature, high power, and high-frequency applications in microelectronics and electro-optical devices.[3–5] Si_3N_4 has received some attention in the last decades, as a potential high-temperature–high-strength structural material.[6] Some of its properties can even be enhanced by SiC in SiC/Si_3N_4-composite materials.[7–9]

There are, of course, kinetically stable CN molecular oligomers; some of them are of great importance in chemistry. Not long ago, considerable excitement was generated by the suggestion of carbon nitride(s), especially C_3N_4, as superhard materials.[10–12] In our opinion, a consensus as to whether the pure material C_3N_4 has or has not been made, has not yet been reached. The development of Si_4C shows the continuing interest in silicon carbon compounds.[13–15]

Amorphous, homogeneous ternary Si-C-N phases are well known. A modern approach for their synthesis is provided by the polymer-to-ceramic-conversion route.[16] These materials, not without impurities of H and O, are in general considered to be thermodynamically metastable, but kinetically persistent at ambient temperatures. Many of them, if not all, will segregate into amorphous SiC, amorphous Si_3N_4, and C, at temperatures exceeding 1000 °C.[17] A ternary crystalline phase, one whose free energy (in theory) would reveal no tendency towards decomposition—at reasonable temperature and pressure—would therefore be noteworthy.

Recently, two crystalline solids in the ternary Si-C-N system, silicon dicarbodiimide (SiC_2N_4) and silicon carbodiimidenitride (Si_2CN_4), have been reported.[18] SiC_2N_4 is obtained by the polycondensation reaction of silicon tetrachloride ($SiCl_4$) with *N,N′*-bis(trimethylsilyl)-carbodiimide (Me_3Si-N=C=N-$SeMe_3$; Me=CH_3) at temperatures between 25 and 100 °C, followed by calcination in vacuum at 350 °C. The initially amorphous white powder crystallizes at about 400 °C to give polycrystalline SiC_2N_4. Once the crystalline compound has formed, it undergoes a reversible phase transformation at about 150 °C. SiC_2N_4 is thermally stable (under Ar) up to 900 °C, when it decomposes to give Si_2CN_4 and the gaseous byproducts cyanogen (C_2N_2) and nitrogen (N_2). Like SiC_2N_4, Si_2CN_4 is also nanocrystalline. While for the former a typical particle size about 10–20 nm can be estimated, crystals of the latter shows a platelike habit with a thickness of 4–10 nm and a lateral extension of 20–70 nm. The process of phase formation, phase transformation, and decomposition has been thoroughly investigated by *in situ* x-ray diffraction (XRD) and thermal gravimetric analysis, with concurrent mass spectrometry.[18]

The crystalline compounds are both examples of covalently bonded carbodiimide moieties in the extended state.

Rewriting their formulas, relations to oxide structures become obvious: $SiC_2N_4 \equiv Si(NCN)_2$, and $Si_2CN_4 \equiv Si_2N_2(NCN)$. And indeed, the proposed structural model for SiC_2N_4 has a resemblance to that of cristobalite-SiO_2;[19] similarly, the topology of Si_2CN_4 is related to that of silicon oxynitride, Si_2N_2O.[20,21] Hence, the -NCN-carbodiimide group plays formally the role of -O- oxygen in these materials. In molecular chemistry, the comparable behavior of the two moieties has been summarized by attributing a *pseudo-chalcogen* character to the carbodiimide moiety.[22] For the compounds this trend is corroborated by the experimental results of ^{29}Si-NMR,[23] and of Si *K*-edge x-ray absorption near-edge structure (XANES),[24] which are very similar to those of their corresponding oxide counterpart.

Nanocrystallinity has stood in the way of a single-crystal structure determination for both compounds. Nevertheless, some topological information could be extracted from the XRD powder-diffraction data using the Rietveld method. However, the structure of the low-temperature phase of SiC_2N_4 could not be determined. Furthermore, many of the interatomic distances computed from the derived positional parameters for the high-temperature phase of SiC_2N_4, as well as for Si_2CN_4, are (as we will see) chemically unreasonable.

Our aim in this work is to give a better description of these crystalline ternary Si-C-N phases and to propose a structure for the low-temperature phase α-SiC_2N_4. Moreover, we want to calculate their free energy to see whether one of these new compounds may be thermodynamically stable. This is done using *ab initio* methods within the framework of density-functional theory (DFT).

The article is organized as follows: In the next section we describe briefly the molecular structure of silylated carbodiimides as well as the crystal structures of the new ternary compounds. For the latter, we discuss the apparent structural inconsistencies, which lead us to propose some alternative structures for SiC_2N_4 and for Si_2CN_4. We then give a description of the procedure for calculating the ground-state structures in both the molecular and the extended state. The presentation is concluded with remarks on the thermodynamics of the system.

STRUCTURAL MODELS

Silylated carbodiimides

Silylated carbodiimides are well known both in molecular chemistry and in materials science—their synthesis, characterization, and thermal stability have recently been reviewed.[25] A convenient reagent for the synthesis of silicon-carbodiimide molecules, polymers, and the new extended structures is N,N'-bis(trimethylsilyl)-carbodiimide (Me_3Si-N=C=N-$SiMe_3$). Its structure has been characterized by single-crystal x-ray diffraction[26,27] as well as by gas-phase electron diffraction.[28] For the smaller sibling N,N'-disilyl-carbodiimide (H_3Si-N=C=N-SiH_3), which we will investigate for computational convenience, only an electron diffraction structure is available.[29] Not long ago, a computational study of H_3Si-N=C=N-SiH_3 was published.[30]

In analogy to the carbodiimide molecule (H-N=C=N-H),[31] we can expect the silylated molecules to adopt C_2 symmetry in their ground state. In Fig. 1 we show the general structure of an Si-N=C=N-Si fragment, as it appears in both the molecular and the extended state.

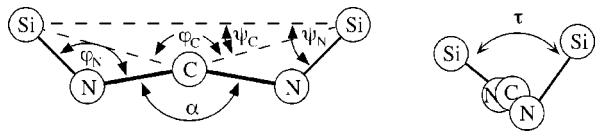

FIG. 1. The Si-N=C=N-Si fragment considered in this paper. The different angles defined here are used for the discussion later on and explained in the text.

The bond angle at the nitrogen (Si-N=C), which we call φ_N throughout the paper, might at first thought to be close to 120° (''sp^2 hybridization at N''). However, a better estimate might be 150°, given the normal opening of angles at N upon substitution by silyl groups. We introduce the angle φ_C (at first sight not an obvious molecular descriptor) to facilitate a comparison to equivalent oxide structures. The two angles ψ_N and ψ_C, purely geometrical descriptors with no obvious chemical significance (as yet), describe the deviation of N and C from the geometrical line Si$\cdots$Si. ψ_C is easily related to φ_C. And ψ_N describes the rotation angle of the SiN_4 tetrahedra in SiC_2N_4, and is relevant in the context of the ''NCN'' — ''O'' analogy. The angle α within the carbodiimide (NCN) group need not be the ideal 180°, since it is not constrained to this value by symmetry. Finally, τ describes the dihedral angle between the two planes defined by the Si-N=C and C=N-Si units. Since the carbodiimide is a heterocumulene, we would expect τ to be near 90°. However, as theoretical calculations show,[30] the barrier to linearity of the whole Si-N=C=N-Si fragment appears to be very low. How this may influence the energetics of extended structures will become clear below.

SiC_2N_4

Using the resemblance of SiC_2N_4 to SiO_2, the proposed structure of SiC_2N_4 may be described as two interpenetrating cristobalitelike networks (see Fig. 2).

Since this is an interpenetrating diamondlike network, a connection to many other compounds is readily made.[32] Like the corresponding oxide system, SiC_2N_4 also exhibits a reversible phase transformation between a low- and a high-temperature modification, which we call accordingly α-SiC_2N_4 (the low-T phase) and β-SiC_2N_4 (the high-T phase).

While the crystal structure of α-SiC_2N_4 could not be determined from the powder data, there is a proposed structure of β-SiC_2N_4, which is cubic [space group $Pn\bar{3}m$ (224)].[18] The atomic positions derived give linear (at N and C) Si-N=C=N-Si fragments in the structure. However, the lattice constant ($a = 6.19$ Å) together with the nitrogen positional parameter ($N_x = 0.147$) leads to too short interatomic distances (Si-N = 1.58 Å, C-N = 1.1 Å). The additional observation of considerable static disorder in the structure led the authors to suggest that the observed structure is an average structure—which again is quite similar to the case of high-cristobalite SiO_2. Assuming reasonable bond distances (Si-N$\simeq$1.7 Å and C-N$\simeq$1.2 Å), and allowing only the N atoms to move out of the threefold axis, would give us a bond angle $\varphi_N \approx 135°$.

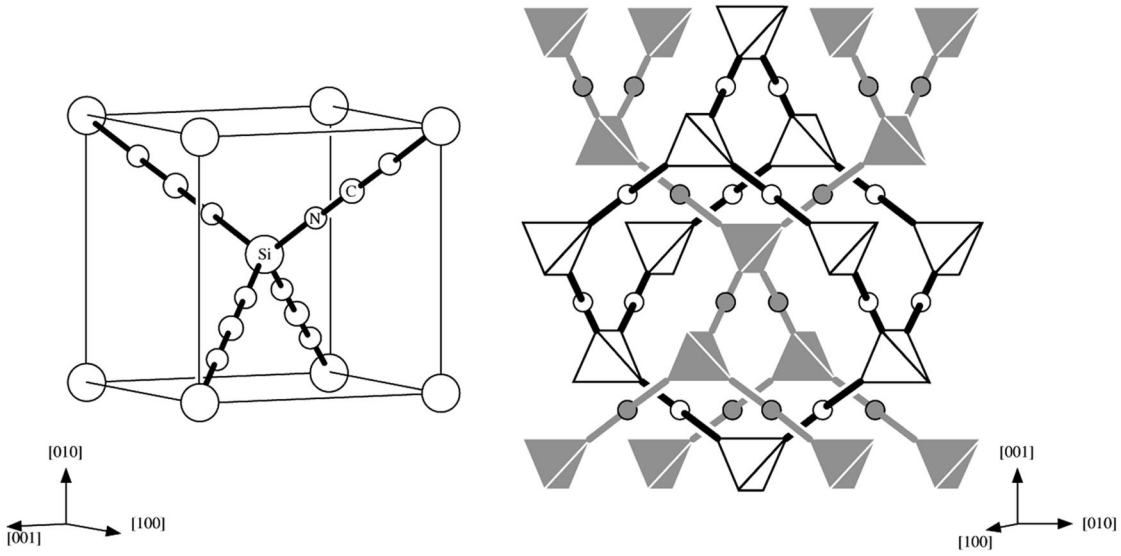

FIG. 2. The proposed (ideal) structure of β-SiC_2N_4 [space group $Pn\bar{3}m$ (224)]. On the left side the unit cell is indicated. On the right we show an extended view showing the interpenetration of two cristobalitelike nets; the four-connected vertices of the network are decorated with SiN_4 tetrahedra, which are linked via bridging C's (small circles).

Since we believe that the cubic structure of SiC_2N_4 merely reflects an average structure, and the positional parameters are approximate, we were in search of candidates for the ''true'' structures of SiC_2N_4. The close resemblance of the silicon dicarbodiimide system to that of silicon dioxide makes it reasonable to seek a structural equivalence or relationship. For low-cristobalite SiO_2 a structure within space group $P4_12_12$ (92) has been established.[33] This was, therefore, our first choice for the low-temperature structure of α-SiC_2N_4.

The story of high-cristobalite SiO_2 is much more complicated. After the original work of Wyckoff,[19] several suggestions for a structure of high-cristobalite SiO_2 were made. The present consensus is that the diffraction pattern is best explained assuming a structure with space group $I\bar{4}2d$ (122); the observation of static disorder gives rise to different explanations, e.g., twinning or domain formation.[34]

How are we going to construct structural models in the SiC_2N_4 system? First, let us assume that the center of the carbodiimide group, the C atom, plays the *positional* role of the oxygen in cristobalite-SiO_2. The utility of this supposition is apparent when we adopt the way of describing cristobalite structures of O'Keefe and Hyde:[35] We can describe the position of C with one rotation angle ψ_C (see Fig. 1) of the SiC_4 tetrahedra—and a first guess of a reasonable value for this angle is readily obtained from the molecular model. But the local coordination tetrahedron of the Si is the SiN_4 tetrahedron. Therefore, we get another rotation angle ψ_N for describing the N position. The additional constraints of reasonable bond distances (Si-N$\simeq$1.7 Å and C-N$\simeq$1.2 Å), as well as the (nearly perfect) linearity of the carbodiimide group, complete the information we need to make a reasonable guess for all internal coordinates. It is thus possible to construct structural models with space group symmetries $P4_12_12$ and $I\bar{4}2d$.

The last task is to make these structures interpenetrate. In principle, there are two independent nets. We have chosen an ''ideal'' interpenetration, which is achieved by a *C* centering of a single net, leading to two identical interpenetrating networks. Our reason for this choice is twofold: for one thing, this is the common interpenetration mode for so many diamondlike networks,[32] and on the other hand, it is a choice of computational convenience. *C* centering of $P4_12_12$ yields $P4_322$ (95), with half the volume in the unit cell. The ''interpenetrating counterpart'' to $I\bar{4}2d$ is found with space group $P\bar{4}n2$ (118). The latter model has the same number of atoms and the same arrangement of the Si atoms as found in the ideal ''average'' structure $Pn\bar{3}m$. Both structures are, although interpenetrating, still very open, with a density of about $\rho\approx 1.5$ g/cm^3.

Si_2CN_4

The structure of Si_2CN_4 consists of layered sheets linked via a carbodiimide group. It can be constructed in the following way: Build up a (planar) sheetlike structure by condensing SiN_4 tetrahedra ($SiN_{3/3}N$ tetrahedra). Three of the four vertices share common corners. The fourth vertex points perpendicular to the plane, half of all of them point up, the other half point down (see Fig. 3). The stoichiometry of this two-dimensional net is SiN_2. The sheets are then linked via a carbon atom at the apical N atoms of the layers. That C and the apical N's form the carbodiimide moiety. Two other ways of constructing the same structure are given in the Appendix, which also includes the description of a third structural variant with a different topology of the SiN_2 layers.

Because the NCN unit is a spacer of substantial size, two different connection patterns between the layers are possible. The proposed structure for Si_2CN_4 in space group $Aba2$ (41), Fig. 4 left, gives an alternating sloping connection between two layers. In contrast, a structure analogous to silicon oxynitride, Si_2N_2O, with space group $Cmc2_1$ (36), exhibits straight parallel connections between the layers (see Fig. 4 right).

The Rietveld refinement procedure to determine the structural parameter for Si_2CN_4 was stable and preserved the to-

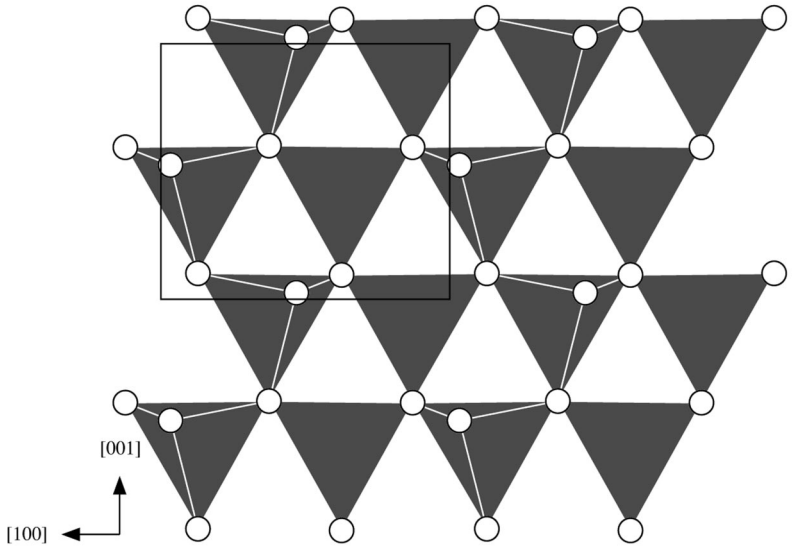

FIG. 3. A single SiN_2 sheet in Si_2CN_4 viewed from the top. Only the vertex atoms of the SiN_4 tetrahedra are shown. Half of the Si and apical N atoms are above the plane, the other half below. The unit cell is outlined.

pology of the model.[18] However, the parameters obtained are rough, since the interatomic distances $d_{\text{Si-N}}$ (1.51–1.89 Å) and angles within the SiN_4 tetrahedron (103.5°–117.2°) are not reasonable. We have chosen to calculate two possible structural models for Si_2CN_4: the one originally proposed with symmetry Aba2, and the ''true'' Si_2N_2O analog, to see whether an alternative connection of the layers might prove energetically favorable. Si_2CN_4 is denser than SiC_2N_4. With $\rho \approx 2.3$ g/cm^3 the density is in-between that of SiC_2N_4 and of Si_3N_4 ($\rho \approx 3.2$ g/cm^3).

THEORETICAL METHOD

Our calculations of the total energy and atomic structures are of the density-functional theory (DFT)-type.[36–39] For molecular properties we used the Amsterdam density functional (ADF) program.[40–42] The valence atomic orbitals were expanded in a set of Slater-type orbitals. For all atoms we used a triple-ζ basis set with two polarization functions (type V).[43] The core shell was treated in the frozen-core approximation.[44] We used the local-density approximation (LDA) as parametrized by Vosko, Wilk, and Nusair.[45] Gradient corrections were applied using the approach of Becke for exchange,[46,47] and of Perdew for correlation.[48] The ADF was run on a Silicon Graphics Power Challenge.

For the extended structure calculations we used the local-density approximation,[49,50] with soft separable,[51] norm-conserving, nonlocal pseudopotentials.[52–54] The electronic wave functions were expanded into plane waves with an energy cutoff of $E_{\text{cut}}^{\text{PW}} = 40$ Ry for preliminary and $E_{\text{cut}}^{\text{PW}} = 80$ Ry for final optimizations. Additional checks were done with $E_{\text{cut}}^{\text{PW}} = 120$ Ry. In the integration over the Bril-

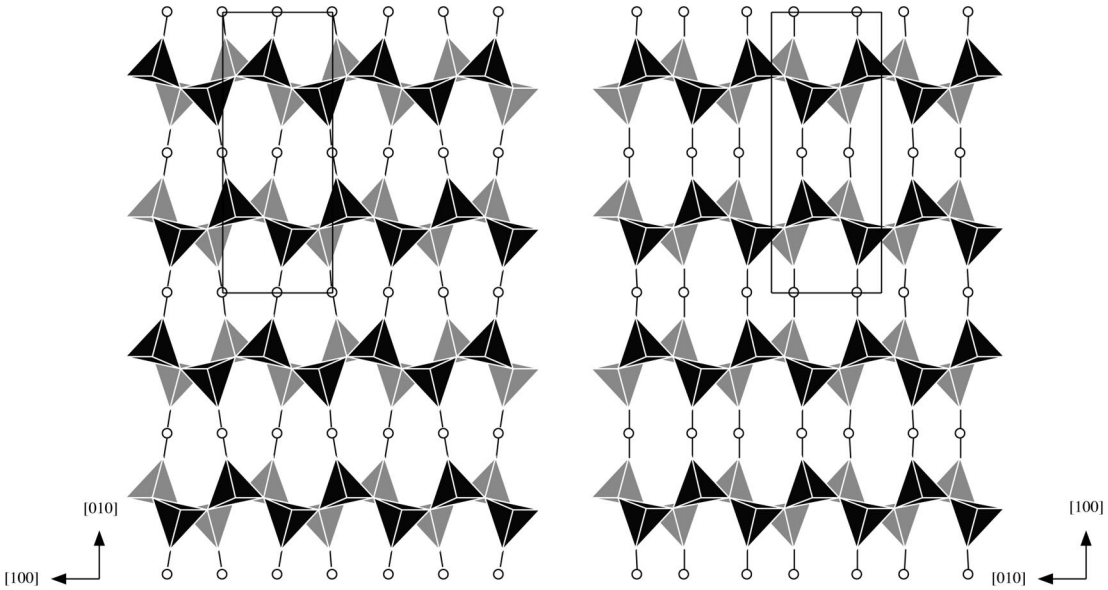

FIG. 4. The two structures we considered for Si_2CN_4. On the left, the candidate with space group $Aba2$ (41), on the right, the $Cmc2_1$ (space group 36) structure. In both cases sheets of condensed SiN_4 tetrahedra are linked via bridging C's. The structures differ in every other SiN_2 layer. We use shading to illustrate the stacking pattern: for the $Aba2$ structure along [001], for the $Cmc2_1$ structure along $[00\bar{1}]$. One unit cell is outlined in each case.

TABLE I. Calculated bond distances and bond angles within the Si-N=C=N-Si fragment for molecules and extended structures. Relevant bond lengths and angles are described in Fig. 1. All distances are in Å, angles in degrees.

	R_3Si-N=C=N-SiR_3		SiC_2N_4		Si_2CN_4	
	R=H	R=CH_3	$P\bar{4}n2$	$P4_322$	$Aba2$	$Cmc2_1$
$d_{Si\text{-}N}$	1.718	1.737	1.668	1.668	1.675	1.674
$d_{C=N}$	1.213	1.216	1.197	1.198	1.196	1.197
φ_N	158.0	152.3	159.1	159.4/164.3	170.9	163.3
α	177.1	176.4	176.9	176.9	178.2	176.9
τ	107.9	99.9	31.8	6.1	12.6	0.2
φ_C	167.7	162.6	159.3	162.0	171.2	163.2
ψ_C	6.2	8.7	10.4	9.0	4.4	8.2
ψ_N	13.6	18.1	19.0	15.5/17.6	8.2	15.2

louin zone we used special points.[55] For the relaxation of the internal coordinates the forces were calculated.[56] A damped Verlet algorithm was used to relax the structure. Here, all calculations were carried out using the program FHI96MD of the Fritz-Haber-Institut in Berlin (Germany).[57,58] The major part of the work was done running the program on nodes of the SP2 of the Cornell Theory Center. Additional calculations were carried out on a Silicon Graphics Power Challenge.

Given the small energy differences associated with angular deformations great care had to be exercised in the optimization. The details are provided in the Appendix.

GEOMETRICAL RESULTS

In this section we discuss the results of our calculations of the geometry of molecular models followed by SiC_2N_4 and Si_2CN_4.

Silylated carbodiimide molecules

For both H_3Si-N=C=N-SiH_3 and Me_3Si-N=C=N-SiMe_3, the optimized geometry had C_2 symmetry (in Ref. 30 the higher symmetry C_{2h} was used). The general structure of the Si-N=C=N-Si fragment can be seen in Fig. 1. In Table I we present the relevant bond lengths and angles, grouped together with those for the extended structures.

The calculated Si-N bond lengths in both molecules are reasonable and significantly shorter (as expected) than the value in a model of $N(SiH_3)_3$ we calculated. Both the SiH_3 and $SiMe_3$ derivatives are slightly bent at N, and the dihedral angle τ in them is not far from 90° expected for allene. There is a tiny deviation from linearity at the central C. Linearizing at both N and C costs very little in energy. However, in both cases the geometry with the higher symmetry has imaginary frequencies, indicating a transition state of higher order. Another impression of the energetics associated with φ_N may be obtained from a plot of the binding energy of H_3Si-N=C=N-SiH_3 as a function of the bond angle φ_N in Fig. 5. The resulting curve shows a very shallow energy surface (high structural flexibility) of the molecule for $140° \leqslant \varphi_N \leqslant 180°$.

Two consequences of this low-energy bending mode are obvious: First, the N atom is easily accessible for electrophilic attack, hardly shielded by the bulky ligand $SiMe_3$. Second, small influences in the environment, for example, crystal packing, impurities, thermal vibrations, may result in large perturbations of the molecular geometry. While the influence of crystal packing or impurities may explain the wide range of values found for φ_N in various crystal structures, the influence of thermal vibrations manifests itself in large vibrational ellipsoid (high-temperature factors) of the nitrogen in crystallographic refinements of silylated carbodiimides.[59,60]

SiC_2N_4

In the previous section we obtained a reasonable picture of the geometry of the Si-N=C=N-Si fragment. The results were then used to build starting configurations for SiC_2N_4. We optimized the geometries of the cubic ($Pn\bar{3}m$) as well as of the tetragonal ($P\bar{4}n2$ and $P4_322$) structures of SiC_2N_4. For the tetragonal structures, we assume from here on an ideal c/a ratio, neglecting possible tetragonal strain. The unit-cell parameters for each structure are given in Table II; the geometries are drawn in Fig. 6.

We can see that there is slight bending at N in both structures. The bond angle α inside the carbodiimide group is almost linear, but deviates from 180° in both cases as in the molecular model. The actual values for relevant distances and angles within the Si-N=C=N-Si fragment, which are collected in Table I, agree very well with the molecular model, except for the $d_{Si\text{-}N}$ bond length.[61] We attribute this discrepancy to the different approximations of the exchange-

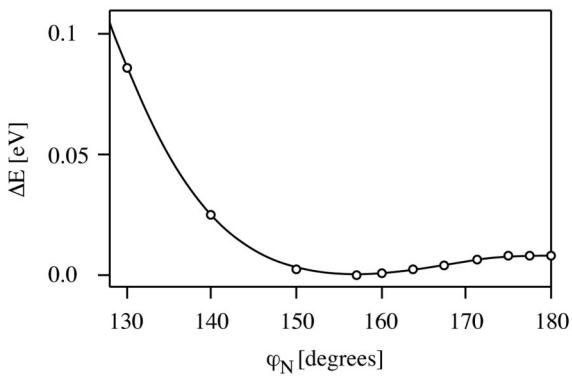

FIG. 5. Relative energy for H_3Si-N=C=N-SiH_3 as a function of the bond angle φ_N.

TABLE II. Crystal structures with internal coordinates (in 10^{-4}) for SiC_2N_4. *W* denotes the Wyckoff position.

Atom	*W*	*x*	*y*	*z*
SiC_2N_4 in $Pn\bar{3}m$ (224) $a=6.59$ Å, $Z=2$				
Si	2*a*	0000	0000	0000
C	4*b*	2500	2500	2500
N	8*e*	1455	1455	1455
SiC_2N_4 in $P\bar{4}n2$ (118) $a=6.38$ Å, $c=6.38$ Å, $Z=2$				
Si	2*a*	0000	0000	0000
C	4*f*	1940	3060	2500
N	8*i*	0746	2011	1498
SiC_2N_4 in $P4_322$ (95) $a=6.35$ Å, $c=12.7$ Å, $Z=4$				
Si	4*a*	0000	6097	0000
C	8*d*	3269	1607	4032
N_1	8*d*	1985	2381	4604
N_2	8*d*	4587	0784	3501

correlation functional utilized for the molecular models (GGA) and for the extended state (LDA).

In Fig. 7 we plot the total energy of the three different candidate structures for SiC_2N_4 as a function of volume. For each volume the internal atomic coordinates are determined by relaxation of the calculated forces.

The implication of the plot is that both tetragonal structures are lower in energy than the ideal cubic structure, leading us to two structural alternatives for SiC_2N_4. The $P4_322$ structure is even more stable than the $P\bar{4}n2$ structure. In comparison to the cubic structure, the total-energy curves for both tetragonal variants show a very shallow energy hypersurface—these compounds appear to be much ''softer.'' If we fit the data in Fig. 7 around the minimum with the Murnaghan equation of state for each curve,[62] we get a measure for the compressibility or its inverse, the bulk modulus *B*. Table III lists the results of the fit for the three different structures of SiC_2N_4. Both tetragonal structures do have a bulk modulus which is about one order of magnitude lower than the value for the ideal cubic structure. For comparison, the calculated value for B_0 of 10 GPa is much lower than that of Si_3N_4 [245 GPa (Ref. 63)] or SiC [220 GPa (Ref. 64)]. Even the value of B_0 in α-cristobalite SiO_2 is about 50% higher than in the $P4_322$ structure.[65]

If we look at the internal bond lengths and angles for the structures at different volumes, we can see why such a shallow energy hypersurface and high compressibility is found. On diminishing the lattice constant from $a=6.6$ Å to $a=6.0$ Å, all bond lengths within the structure remain essentially constant. The tetrahedral angles around the silicon, as well as the bond angle α at the C inside the carbodiimide group, also retain their nearly ideal values of $\approx 109.5°$ and $\approx 180°$, respectively. The geometrical parameter which varies significantly is the bending angle at N, φ_N, and, of course, the angles within the Si-N=C=N-Si fragment related to it. φ_N decrease continuously from 180° at $a=6.6$ Å to about 140° at 6.0 Å for both tetragonal structures. Thus, it takes very little energy to rotate the SiN_4 tetrahedra. Or, to take another perspective: the shallow energy hypersurface suggests the posssibility of low-energy phonon modes in the lattice, which eventually lead to a negative contribution to the thermal-expansion coefficients. An exceptional example of this phenomenon is the flexible network of ZrW_2O_8.[66]

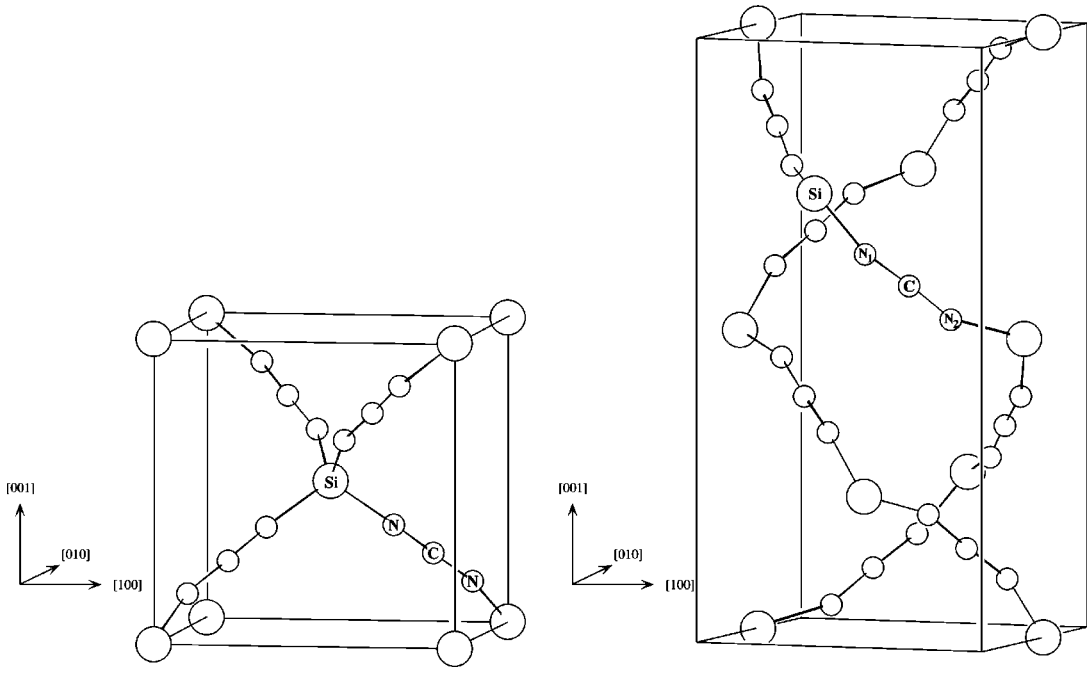

FIG. 6. The unit cell of $P\bar{4}n2$ SiC_2N_4 (left side) and of $P4_322$ SiC_2N_4 (right).

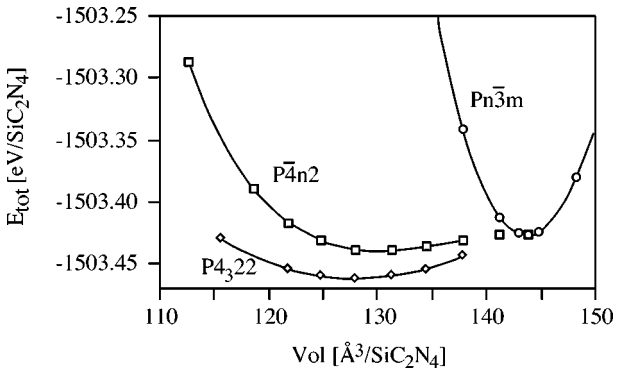

FIG. 7. Plot of the total energy as a function of the volume for the three investigated structures of SiC_2N_4. For each volume the internal coordinates were relaxed. The lines correspond to fits to the Murnaghan equation of state.

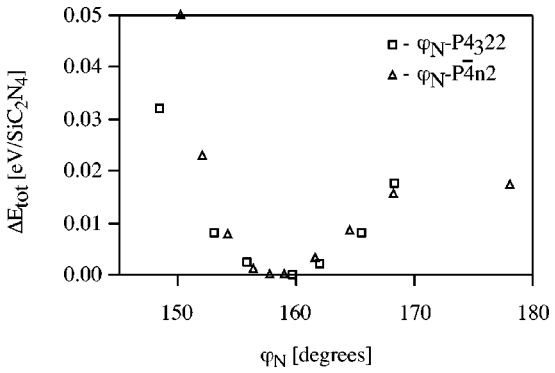

FIG. 8. Plot of the relative total energy (zero at the lowest energy geometry) as a function of the bond angle φ_N for the structures of $P\bar{4}n2$ and $P4_322$. φ_N was extracted from optimized geometries obtained for a given volume. For $P4_322$ we have averaged over φ_{N_1} and φ_{N_2}.

To further demonstrate the close relation between molecules and extended structures we took from the optimizations of Fig. 7 the angle φ_N at nitrogen at which the total energy for a given volume is minimized. A comparison of the resulting plot shown in Fig. 8 with Fig. 5 shows a close resemblance of the two curves. The plots in Fig. 8 show us the contribution of the ''nitrogen bending potential'' to the total energy, since all other geometrical parameters are almost constant. As in the molecular case, this plot reveals the high flexibility of φ_N—quite similar to the bond angle at the O in so many structures of SiO_2.[67]

Looking again at the results in Table III we observe that the energy differences between the phases we calculated are very small, of the order of 13–40 meV (1–4 kJ/mol) per formula unit. While the values *per formula unit* are about the same as those calculated and observed in cristobalite SiO_2,[65] the energy differences *per atom* (2–6 meV) are at the limit of our precision. To gain some confidence in our results we doubled both the $Pn\bar{3}m$ and $P\bar{4}n2$ structures along the c axis, so as to facilitate a direct comparison with the $P4_322$ structure. The calculations were carried out using (the same) $6\mathbf{k}$ points and $E_{cut}^{PW}=80$ Ry in each case. The energy differences were identical. Moreover, we computed the path by which the structure with the ideal setting within cubic space group $Pn\bar{3}m$ distorts into the structure with tetragonal space group $P\bar{4}n2$.[68] The results for various lattice constants between 6.6 and 6.2 Å, corresponding to different volumes, indeed fit very well into the plot of Fig. 7. All internal coordinates change nearly linearly with increasing pressure. These results, the comparison in a common tetragonal setting, and the tracing of the distortion path, substantiate that the $P\bar{4}n2$ and the $P4_322$ structures are indeed lower in energy than the $Pn\bar{3}m$, and that we can trust these admittedly tiny energy differences.

TABLE III. Results of fitting the total-energy calculations for SiC_2N_4 to the Murnaghan equation of state. The volume is given per SiC_2N_4 formula unit. The energy difference is given in eV per formula unit relative to the ideal arrangement in $Pn\bar{3}m$. The values (a, B_0, and ΔE) are not significantly influenced if B' is fixed to 4 in the fitting.

Space group	$Pn\bar{3}m$	$P\bar{4}n2$	$P4_322$
a (Å)	6.6	6.39	6.35
c/a	1	1	2
V_0 (Å^3/SiC_2N_4)	143.7	130.3	128.0
B_0 (GPa)	108	8.5	7.9
B'	3.7	16	1
ΔE (eV/SiC_2N_4)	0	−0.013	−0.040

But did we find the right structure for α-SiC_2N_4? We do not really know, since our calculations cannot match the experimental lattice constant, which is 6.19 Å. Nevertheless, the resemblance of the proposed structure for SiC_2N_4 to cristobalite-SiO_2 is striking. Let us, therefore, discuss further the lattice constant. The value computed for the ideal $Pn\bar{3}m$ structure, 6.6 Å, is about 6% too high. But even the structure with lowest energy, the $P4_322$ structure (which satisfies expectations based on the molecular structure) has a lattice constant $a=6.35$ Å, which is 2.5% off the experimental value. Although this does not look bad, it goes against the trend of the LDA overestimating bonding; the lattice constants of semiconductors such as Si or SiC are usually computed a bit too small. In our calculations we saw that the experimental lattice constant of 6.2 Å may correspond to a bond angle φ_N of 150°, which is a completely reasonable value.[26,27,60]

There are two possible solutions to this puzzle: First, as we pointed out already for the molecular models, the nitrogen bending angle φ_N is very sensitive to changes in its environment. Therefore, our model of the crystal structures of SiC_2N_4 might be right, and the experimental results may be due to impurities and defects, as well as to the size of the crystals, which may all influence φ_N. Second, although within the methodology we use we can be certain of the energy differences we compute, the functional chosen to calculate the total energy may also influence significantly the topology of this inherently shallow energy hypersurface.

The challenge posed to theory by the structure is considerable. Whatever the explanation of this one discrepancy may be, we think that the results we present clearly show that the ''true'' structure of SiC_2N_4 is not the proposed cubic one, but very probably one of tetragonal symmetry. Following through the resemblance to the cristobalite-SiO_2 system,

TABLE IV. Unit-cell description with internal coordinates (in 10^{-4}) calculated for structures of Si_2CN_4 (left and middle). For comparison the experimental values of Ref. 18 (right). $Z=4$ for all structures. The Wyckoff positions are $4a$ for C, and $8b$ for the other atoms (the same in both space groups).

	Calculations						Experiment		
	Si_2CN_4 in $Aba2$ (41)			Si_2CN_4in $Cmc2_1$ (36)			Si_2CN_4 in $Aba2$ (41), Ref. 18		
a (Å)	5.45			13.86			5.44		
b (Å)	13.81			5.45			13.58		
c (Å)	4.82			4.79			4.81		
Atom	x	y	z	x	y	z	x	y	z
Si	0985	2029	9542	2029	1523	3029	1010	1970	9390
C	0000	0000	0000	0000	2128	2535	0000	0000	0000
N_1	8728	2697	1099	2294	1234	6490	9070	2600	0670
N_2	0390	0852	0038	0863	2173	2490	0290	0760	0000

we can furthermore distinguish between two possible phases of SiC_2N_4. Therefore, we feel confident in proposing a crystal structure for the low-temperature modification (α-SiC_2N_4), namely the $P4_322$ structure, which is analogous to the low-temperature modification of cristobalite. The $P\bar{4}n2$ structure may eventually serve as a model for the high-temperature modification, β-SiC_2N_4.

Si_2CN_4

Both structural candidates for Si_2CN_4 turned out to be very similar and close to each other in energy. At $E_{\text{cut}}^{\text{PW}}=40$ Ry the $Cmc2_1$ structure is favored over the $Aba2$ structure by ≈ 10 meV per Si_2CN_4 unit (≈ 1 kJ/mol). The preference is reversed for calculations with $E_{\text{cut}}^{\text{PW}}=80$ Ry and $E_{\text{cut}}^{\text{PW}}=120$ Ry. As we pointed out before these values are at our limit of precision. Therefore, we do not think that these differences are as significant as those of various structures in the SiC_2N_4 system; we regard the $Cmc2_1$ structure as a real alternative.

The optimized geometries for both candidate structures of Si_2CN_4 are described in Table IV, together with the experimental results.[18] The relevant values for the geometry of the Si-N=C=N-Si fragment in the structures are summarized in Table I.

We immediately see that both candidate extended structures have approximately the same lattice constants. Indeed, as a detailed comparison shows, the SiN_2-layered sheets in both structures are nearly identical.

There are some differences in the interlayer connections in the $Aba2$ and $Cmc2_1$ variants. First, our lattice constant in the direction perpendicular to the layers is again too large (as for SiC_2N_4), this time by 1.5%. Second, the fragment in $Aba2$ is much more ''stretched out'' (compare φ_C). Although these differences are there, they obviously do not affect the preference for the $Aba2$ structure. The geometries of both structures are mainly driven by the energetics of the SiN_2-layered sheet. The carbodiimide moiety is flexible enough to connect these sheets in either way.

Why are the SiN_4 tetrahedra ''rotated''? It is impossible to retain the planarity at N that the NSi_3 unit seeks, and yet keep all the N_1 atoms in an ideal planar 3^6 net. In a compromise, the SiN_4 tetrahedra rotate; the rotation also causes the c/a ratio to increase by 2% from its ideal value of $\sqrt{3}/2$.

An interesting subject for further investigation is the different Si-N bonds we can find in the structure of Si_2CN_4. Since both structures are so similar, let us discuss the situation in the $Aba2$ structure, for which we draw the (slightly extended) unit cell in Fig. 9. One of the four bonds of the Si is from Si to the apical N (N_2), which is part of the carbodiimide moiety. The other three are bonds from Si to N's (N_1) inside the layer. While N_2 is only 2 connected, N_1 is 3 connected and almost trigonal planar (angles: 118.6°, 123.7°, 117.1°; $\Sigma=359.4°$). The Si-N_2 bond length then is shorter by 2% than the ''normal'' Si-N_1 bond length in this compound ($d_{\text{Si-N}_2}=1.675$ Å, $d_{\text{Si-N}_1}=1.708$, 1.711, 1.715 Å),

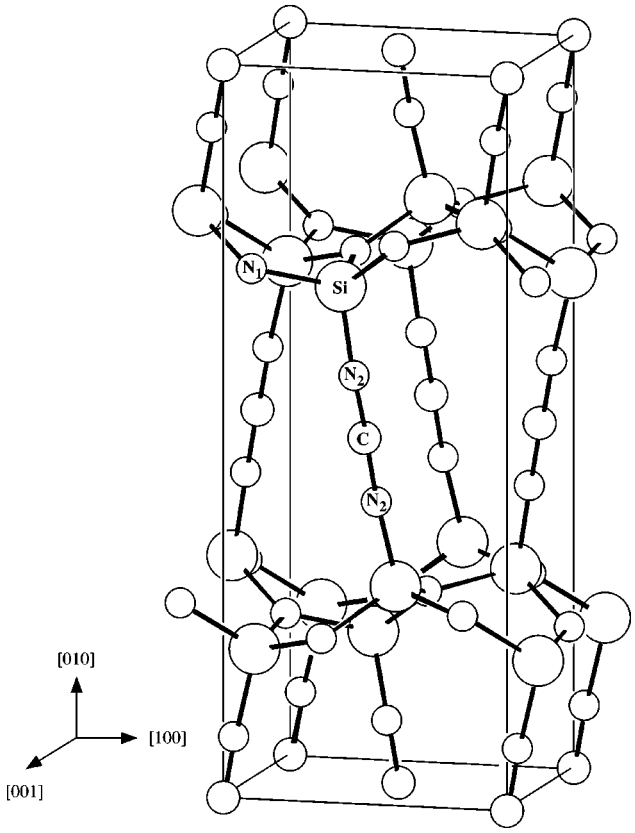

FIG. 9. The unit cell of $Aba2$-Si_2CN_4. We included some atoms outside the unit cell so as to make the connection pattern between atoms visible.

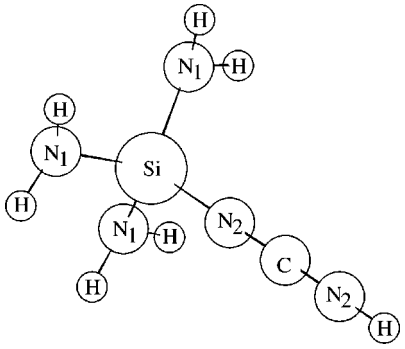

FIG. 10. The model of $(H_2N)_3Si\text{-}N{=}C{=}N\text{-}H$, which serves as a molecular model for the $N_3Si\text{-}N{=}C{=}N$-fragment in Si_2CN_4.

so we may expect slightly different bonding. However, variations like this are likely insignificant, since for $\alpha\text{-}Si_3N_4$ we computed very similar variations (shortest $d_{\text{Si-N}} = 1.706$ Å, longest 1.737 Å).

There may be real consequences of such a bond shortening. Consider the simple molecular model of SiH_4, whose symmetry is reduced from T_d to C_{3v}, if we vary the bond length for one ligand, say $Si\text{-}H_1$. The bonding t_2 set of orbitals then splits into a_1 and an e_1 set; the a_1 comes below the e_1, if the bond length is shortened. Let us define the z axis as the direction of the $Si\text{-}H_1$ bond. Only Si_{p_z} can then mix into the a_1 component. Thus prepared we can analyze the more complicated orbital pattern of the larger molecular model. Consider $(H_2N)_3Si\text{-}N{=}C{=}N\text{-}H$, which serves us as a molecular model for the fragment of the structure of Si_2CN_4 (see Fig. 10). For this model we can identify the relevant a_1 orbital which has a reasonable admixture of Si_{p_z}. We can then compare its energy with that of the orbitals of the e_1 set with substantial $Si_{p_{xy}}$ character. The splitting we find is about 2 eV, quite a big value. The signature of this difference in orbital energies is a doublet structure in the Si K-edge XANES spectrum of Si_2CN_4, which reveals quite different (by 2 eV) (unoccupied) Si p-like states.[24] Of course, in this model the shortening of the bond length is not the only perturbation of the ideal SiN_4 tetrahedra; probably more important is the very different ligand.

For a thorough structure investigation the calculation of elastic constants is indispensable. Like a frequency analysis for molecules, it confirms whether the structure is a local minimum on the energy hypersurface, or if there are distortion modes possible which will lower the total energy of the structure. We examined the elastic constants for Si_2CN_4, which has, since it is orthorhombic, nine independent entries in the elasticity tensor.[69] Six of them are related to compressive stress, three to shear stress. From the way we searched for the correct lattice constants (a,b,c), we can be sure that all elastic constants related to compressive stress will behave properly. The determination of c_{55} turned out to be unproblematic, since it is the shear within the layered sheets,[70] requiring much strain energy. In comparison, the calculation of c_{44} and c_{66} was demanding; in the end both turned out to be very small, but positive. This is understandable, since shearing the layers against each other more or less affects only the connecting carbodiimide unit, which in turn is very flexible.

ELECTRONIC STRUCTURE

Silylated carbodiimide molecules

Let us briefly analyze the orbital pattern of $H_3Si\text{-}N{=}C{=}N\text{-}SiH_3$. The molecule adopts C_2 symmetry; thus we have the irreducible representations A and B to describe the symmetry of the molecular orbitals. Let us divide the molecule into the carbodiimide moiety and the silyl groups. The fragments now have a low symmetry, but their distortion from higher local symmetries, C_{3v} for the SiH_3 fragments and $D_{\infty h}$ for NCN, is only small. To facilitate our description of the molecular orbitals, let us use the fragment orbitals of the (approximately) higher symmetry fragments.

In Fig. 11 we draw the molecular orbitals of $H_3Si\text{-}N{=}C{=}N\text{-}SiH_3$. (See also the orbitals of the parent compound H-NCN-H drawn in Ref. 71.) Core orbitals are omitted. In our picture we have consistently suppressed small contributions ($<10\%$) of fragment orbitals for clarity. Orbital **1a** is virtually identical to the $1\sigma_g$ orbital of the NCN fragment, which we call $1\sigma_g^{(\text{NCN})}$. Together with **1b**, which is almost completely of $1\sigma_u^{(\text{NCN})}$ character, it describes the N-C σ bonds within the NCN unit. **2a** is made up of $2\sigma_g^{(\text{NCN})}$ and of the bonding combination of the $1a_1$ orbitals on the SiH_3 fragments; **2b** mixes the $2\sigma_u^{(\text{NCN})}$ orbital and the out-of-phase combination of the $1a_1$ orbitals on the SiH_3 fragments. The same approximate decomposition holds for the **3a** and **3b** molecular orbitals. These combinations of a_1 orbitals of the SiH_3 fragments with NCN fragment nonbonding $2\sigma_g^{(\text{NCN})}$ and $2\sigma_u^{(\text{NCN})}$ orbitals are Si-H and Si-N bonding. In orbitals **4a** and **4b** we begin to see the π system of the carbodiimide moiety ($\pi_u^{(\text{NCN})}$). Orbitals **5a**, **5b** and **6a**, **6b** are the other components of the σ bonding within the SiH_3 units. The topmost orbitals **7a** and **7b** are made up mainly of the $\pi_g^{(\text{NCN})}$ set and are strongly localized on the N atoms (''N lone pairs''). All in all, these orbitals make chemical sense.

SiC_2N_4

On the left side of Fig. 12 we show the calculated band structure for SiC_2N_4 in the $P\bar{4}n2$ structure. The bands are quite flat and there is not much dispersion anywhere. This is consistent with pretty isolated molecularlike units that are not conjugated. The 32 occupied bands are separated from the unoccupied bands by a band gap of 4.2 eV (LDA) at the Γ point. Since the band structure of the $P4_322$ structure will not look different at all, we do not present it.

Following the analysis of the molecular orbitals of $H_3Si\text{-}N{=}C{=}N\text{-}SiH_3$ drawn in Fig. 11, it is easy to rationalize the band structure of $P\bar{4}n2\text{-}SiC_2N_4$. Thus, the lowest eight bands descend from ''$1\sigma_g^{(\text{NCN})}$'' and ''$1\sigma_u^{(\text{NCN})}$'' orbitals located within the carbodiimide fragments (we have 4 NCN groups). The next eight crystal orbitals (2+6) are ''$2\sigma_g^{(\text{NCN})}$'' and ''$2\sigma_u^{(\text{NCN})}$,'' obviously with admixtures of Si orbitals ($3s$), which cause the splitting. The third set of eight orbitals are then the ''$\pi_u^{(\text{NCN})}$,'' and the fourth set are the ''$\pi_g^{(\text{NCN})}$'' orbitals (N lone pairs). The Si $3p$ states will mix mainly into the latter ''$\pi^{(\text{NCN})}$''-like states.

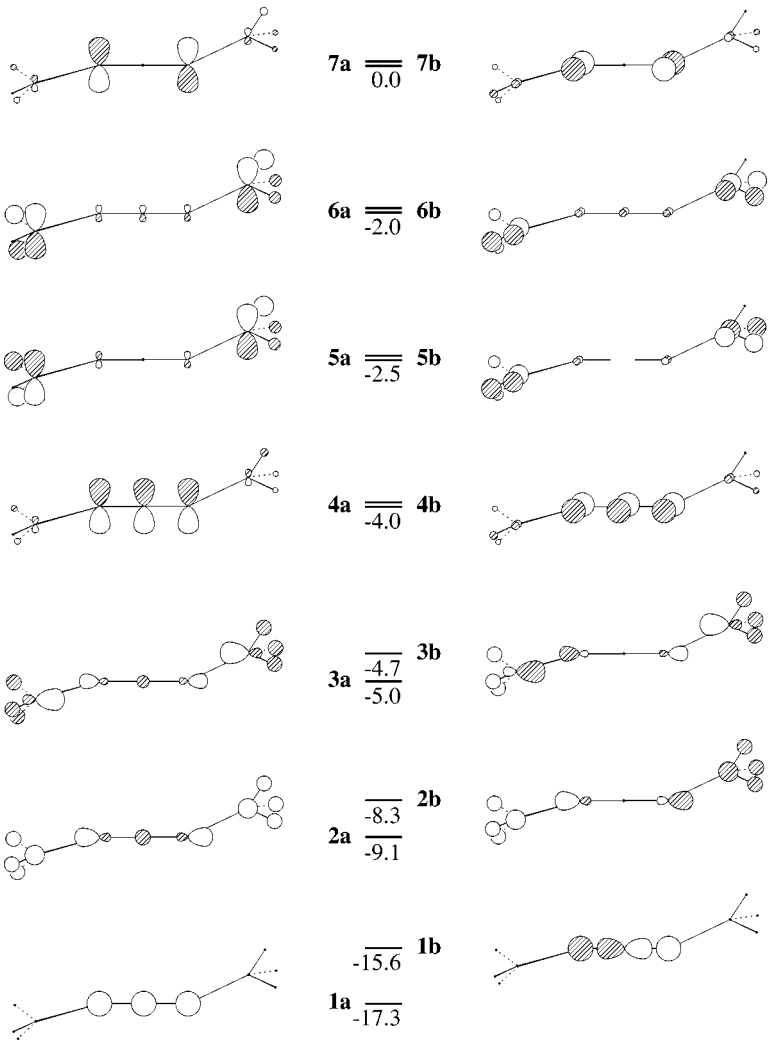

FIG. 11. The molecular orbitals of $H_3Si\text{-}N{=}C{=}N\text{-}SiH_3$. The energy of the orbitals is given in eV relative to the highest-occupied molecular orbital (HOMO) (**7b**). For the HOMO we calculated an orbital energy of -6.6 eV. The orbitals **4a-b**, **5a-b**, **6a-b**, and **7a-b** are approximately degenerate.

Si_2CN_4

The band structure of $Aba2$-Si_2CN_4 is shown on the right side in Fig. 12. There are 64 occupied bands and we included the first four unoccupied states too, which are separated by a direct band gap of 4.2 eV (LDA). The band gap occurs on the way from Γ to X. Due to the large number of bands the picture naturally shows only small dispersion for individual bands. But it can be seen that some dispersion occurs for **k** vectors which are in-plane, while bands running perpendicular to the SiN sheets (see $\Gamma \rightarrow K$ or $L \rightarrow X$) are almost flat.

As in the case of the band structure of SiC_2N_4 (at the left side), we can make out states that are mainly within the carbodiimide group.[72] The lowest 16 bands of the valence band are separated by an ionicity gap (3.4 eV) from the upper part. Within the lower part there is more structure. The lowest eight flat bands are again mainly ''$1\sigma_g$'' and ''$1\sigma_u$''-like states located within the carbodiimide fragments (we again have four NCN groups). The other eight bands are mainly the $2s$-like states of the N_1 atoms. The bottom of the upper part of the valence band consists of eight mainly ''$2\sigma_g$'' and ''$2\sigma_u$'' (carbodiimide)-like states. There is a small gap of 0.6 eV separating these states from the rest of the upper part. The ''π_u''-(NCN)-like states we can find at around -5 eV, and as before, ''π_g'' orbitals of the NCN-group together with $2p$-like states of N_1 are found at the top of the valence band, forming the ''N lone pairs.'' The orbitals of Si mix somewhat into all of these levels.

THERMODYNAMICAL CONSIDERATIONS

Concluding our investigation of the ternary phases, we return to one aspect of the motivation for this study: Are SiC_2N_4 and/or Si_2CN_4 stable phases in the Si-C-N phase diagram? We cannot answer this question, because we are unable to calculate their stability at ambient temperatures and pressures. The meaningfulness of our results is limited to the energy of their structures, and we can hardly leave absolute zero. Nevertheless, a calculation can provide strong evidence for the thermodynamical stability or instability, if only the difference in the calculated free energy is big enough. Therefore, let us take a look at possible decomposition reactions for $SiC_2N_4$and Si_2CN_4.

The observed decomposition reaction of SiC_2N_4, yielding Si_2CN_4, N_2, and C_2N_2, was described in the Introduction. Annealing Si_2CN_4 at temperatures above 1000 °C results in a continuous loss of nitrogen gas (N_2), yielding an amorphous Si-C-N material, which crystallizes at about 1500 °C to form a polycrystalline α-Si_3N_4/α-SiC powder.[18] However, considering the thermodynamic stability of both compounds we have to calculate the free energy with respect to what are believed to be thermodynamically stable phases, namely Si_3N_4, SiC, C, and N_2. This gives us the following

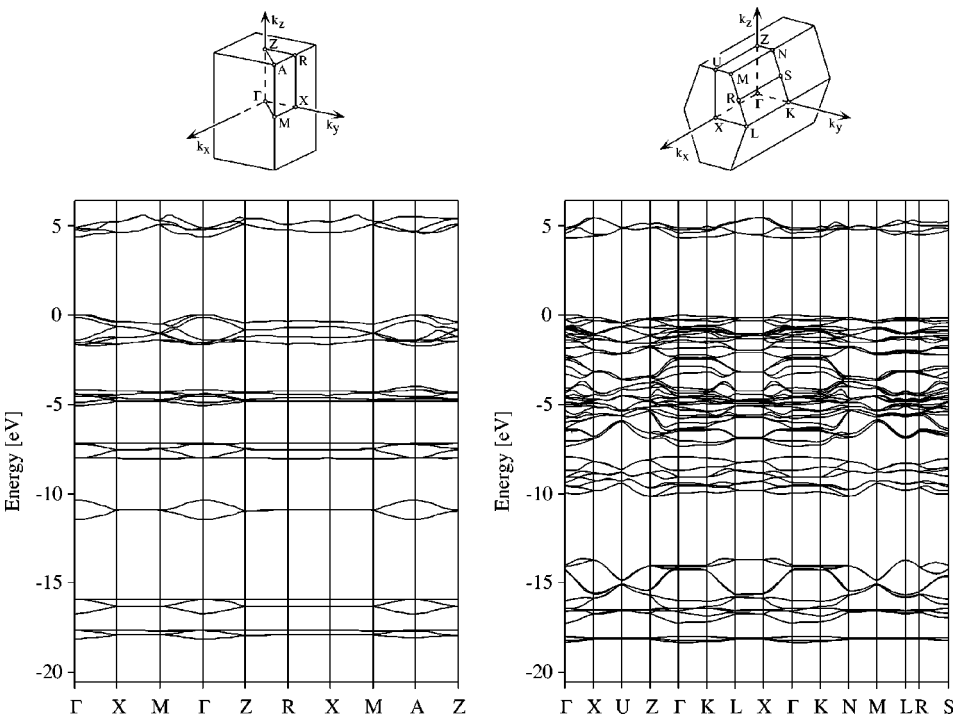

FIG. 12. Left side: Band structure for SiC_2N_4 in $P\bar{4}n2$. Indices label points of high symmetry in the Brillouin zone of the primitive tetragonal lattice, which is outlined on top of the graph. Right side: Band structure of Si_2CN_4 in $Aba2$. Indices label points of high symmetry in the Brillouin zone of the *A*-centered orthorhombic lattice, which is given on top. In both graphs the energy is given relative to the Fermi level which is defined as the top of the valence band.

reactions to consider for SiC_2N_4:

$$SiC_2N_4 \rightarrow \frac{1}{3}Si_3N_4 + 2C + \frac{4}{3}N_2 \tag{1}$$

and

$$SiC_2N_4 \rightarrow \frac{1}{2}Si_2CN_4 + \frac{3}{4}C_2N_2 + \frac{1}{4}N_2. \tag{2}$$

For Si_2CN_4 we look at the reactions:

$$Si_2CN_4 \rightarrow \frac{2}{3}Si_3N_4 + C + \frac{2}{3}N_2 \tag{3}$$

and

$$Si_2CN_4 \rightarrow \frac{1}{3}Si_3N_4 + SiC + \frac{4}{3}N_2. \tag{4}$$

We calculated, using the same method, total energies for β-Si_3N_4, β-SiC, diamond C, and the molecules N_2 and C_2N_2, all at optimized geometries. We subtracted the calculated values from those of the ternary phases following Eqs. (1)–(4), neglecting contributions of zero-point vibrational energies. We note here that all values of ΔH we estimate are one order of magnitude bigger than the computed differences in total energy between the structural candidates. We estimate then the free energy (per formula unit) for reaction 1 to be $\Delta H_1 = -1.1$ eV (-106 kJ/mol), and $\Delta H_2 = +1.8$ eV ($+171$ kJ/mol) for reaction 2. Likewise $\Delta H_3 = -0.4$ eV (-39 kJ/mol), and $\Delta H_4 = +2.4$ eV ($+232$ kJ/mol). The cohesive energies estimated are $E_{coh} = 48.2$ eV for SiC_2N_4 and $E_{coh} = 48.0$ eV for Si_2CN_4 (for comparison $E_{coh} = 47.5$ eV for β-Si_3N_4). The results suggest that both ternary compounds may not be thermodynamically stable. However, as a consequence of the small values of energy differences a definitive assessment of the stability of Si_2CN_4 is impossible. Interestingly, both phases decompose through the energetically unfavored (at $T = 0$ K) channel. Entropy and kinetic factors must influence this outcome. Nevertheless, the calculated cohesive energies suggest the formation of these phases under favorable conditions.

SUMMARY

The flexibility of the Si-N=C=N-Si fragment is the leitmotif of this paper and of our calculations. The very shallow energy hypersurface associated with the Si-N=C bond angle φ_N dominates our considerations of the extended structures of $Si(NCN)_2$ and $Si_2N_2(NCN)$. We propose a crystal structure for α-SiC_2N_4, in analogy to the low-temperature modification of cristobalite-SiO_2. This structure is about 40 meV ($\sim$4 kJ/mol) lower in energy than the ideal cubic arrangement. A second polymorph lies in between these two and may be the structure of the high-temperature modification of SiC_2N_4. For both variants of SiC_2N_4 the calculated bulk moduli of about 8 GPa ($\sim$0.13 Mbar) are remarkably small for a nonoxide covalently bonded material.

Within the Si_2CN_4 system we found two structures nearly equal in energy. One of them corresponds to the experimentally determined $Aba2$ structure, for which we refined the crystal structure. Both structures differ in the connection pattern of the layered SiN_2 sheets. Such geometrical freedom is the consequence of the extension and the flexibility of the carbodiimide unit. In both structures there is a difference between bonds Si-N_1(-Si) and Si-N_2(=C=N) which results in a considerable reorganization of the local orbital pattern at Si.

In all structures the bond angle φ_N is nonlinear, calculated to be 158° in α-SiC_2N_4 and 171° in Si_2CN_4. Some lattice constants we computed (a, c for α-SiC_2N_4, b for $Aba2$-Si_2CN_4) are about 2% too large. We do not know whether this discrepancy derives from the nanostructure of the crystalline phases, including defects, or if it is to be

traced to the LDA functional chosen. The band structure of SiC_2N_4 and Si_2CN_4 exhibits localized states within the carbodiimide moiety, well separated in energy from each other.

We hope this paper will stimulate some future synthetic work on extended carbodiimide structures. Especially, we encourage the reinvestigation of the crystal structures of SiC_2N_4 and Si_2CN_4. For both compounds a determination of the enthalpy will be of considerable interest for thermodynamics in the ternary Si-C-N system.

ACKNOWLEDGMENTS

The authors gratefully acknowledge the generous support by the National Science Foundation (Grant No. CHE 94-08455) and the Center for Materials Science at Cornell University. We also thank the Deutsche Forschungsgemeinschaft, Bonn, (Germany) for financial support through Contract No. Kr 1805/1-1. We thank the Cornell Theory Center for computer time. We acknowledge especially the theory group at the Fritz-Haber-Institut in Berlin/Germany for making their programs publicly available. R.R. thanks the Deutsche Forschungsgemeinschaft, Bonn, (Germany) for research Grant No. Ri 510/3-2 and the Fonds der Chemischen Industrie, Frankfurt, Germany, for financial support.

APPENDIX

Alternative ways of describing Si_2CN_4

Another (second) way of describing the structure of Si_2CN_4 starts from the wurtzite structure and is derived from consideration of the structures of Si_2N_2O and high-pressure boron sesquioxide B_2O_3-II.[73] If we take the wurtzite structure and discard 1/3 of all anion positions, we arrive at an idealized version of B_2O_3-II. The structure becomes sheetlike and the sheets are linked through bridging oxygens. An additional rotation of the BO_4 tetrahedra yields the real structure.[74] Si_2N_2O is isostructural to B_2O_3-II. It is built up from Si_2N_2 sheets and bridging oxygens. If, as we did before with SiC_2N_4, we simply replace the oxygen by a carbodiimide group, we get an alternative [space group $Cmc2_1$ (36)] to the proposed structure of Si_2CN_4 (see Fig. 4 right). This is a structural variant, since in the proposed structure for Si_2CN_4 [space group $Aba2$ (41)] (Fig. 4 left) each second layer is shifted by [1/2,0,1/2] (using crystal coordinates and taking a nonstandard setting $Bba2$), which gives an alternating sloping connection between two layers rather than a straight parallel one as in the $Cmc2_1$ structure.

A third way to build up the structure is by starting from a 6^3 net. As for borazine, we color it in an alternating way with Si and N, its stoichiometry becoming SiN (or Si_2N_2). The Si atoms in this net are then lifted above and below the plane in a concerted way so that the two-dimensional structure becomes wavelike (1 up, 1 down) looking along the *x* direction (see Fig. 3). Equivalent nets are stacked along the *y* axes, every other one shifted by [0,1/2,1/2] (the *A* centering), and finally connected by a carbodiimide group. Since there was no shift along the *x* direction, the wavelike feature causes the alternately sloping connection of the layers. The carbodiimides are orientated along the (110) and $(\bar{1}10)$-directions (see Fig. 4 left).

This third way of constructing Si_2CN_4 actually leads to a third structural alternative, as follows: lift the Si atoms of the Si_2N_2 net in such a way that along the *x* axis they all point in the same direction (either all up, or all down). Along the *y* axis the orientation of the corner-connected SiN_4 tetrahedra could alternate (compare the result with Fig. 3). The optimized geometry has space group $Imm2$ (44), with $a=2.91$ Å, $b=13.86$ Å, $c=4.66$ Å, and $Z=2$. However, the energy of this third structure is 0.3 eV (29 kJ/mol) per formula unit, higher in comparison to the other structures described.

Optimization procedure

For both molecules, $H_3Si\text{-}N{=}C{=}N\text{-}SiH_3$ and $Me_3Si\text{-}N{=}C{=}N{-}SiMe_3$, the geometry was optimized assuming C_2 symmetry. To reach a geometry with no imaginary frequencies, the convergence limits for remaining gradients had to be set to 10^{-4}, the precision for the integration to 6.0 (for frequencies 8.0). Additional optimizations were done for the higher D_{3d} symmetry. A frequency calculation was performed for the optimized geometry of $H_3Si\text{-}N{=}C{=}N\text{-}SiH_3$ to ensure that is is a true minimum. The optimized geometry of $Me_3Si\text{-}N{=}C{=}N\text{-}SiMe_3$ could not be subjected to a frequency analysis since it has too many degrees of freedom.

The extended structures were optimized with the following procedure: Since the FHI96MD program cannot optimize internal parameters and cell constants at the same time, we used an iterative scheme to find the optimum values for the lattice constants. For this we changed the lattice constants stepwise by typically 0.1 bohr, and searched the energy hypersurface for the minimum, allowing a full relaxation of the atomic coordinates in every step. In these preliminary optimizations we used a plane-wave basis with $E_{\text{cut}}^{\text{PW}}=40$ Ry. Generation of the **k** points was done with a [2,2,2] grid for the SiC_2N_4 structures leading to one special **k** point and a [2,4,2] grid for the Si_2CN_4 structures leading to two special **k** points.[70] Using the finer grid along the [010] direction (perpendicular to the layers) accounted better for the sheetlike structure.

The atomic coordinates were considered to be relaxed if the forces were below 5×10^{-5} har/bohr ($\approx 3\times10^{-3}$ eV/Å). However, we observed the following for the tetragonal structures of SiC_2N_4: while in the course of the optimization procedure the total energy often seemed to have converged (absolute changes smaller 10^{-5} a.u.), additional minimization of the forces (typically $<5\cdot10^{-5}$ a.u.) took much longer and could not be achieved in all cases. Quite often we did more than 100 steps in a relaxation. As a consequence, atomic displacements are observed even at a stage where the total energy appears to be minimized. In cases where we could not minimize the forces completely due to ''back-and-forth'' moving of the atoms around a presumed minimum, we took the atomic displacements during the last 20 steps of the iteration as a measure (<0.1 pm) of convergence.

After having gained a reasonable picture of the energy hypersurface of the structures, it turned out to be necessary to increase our basis to $E_{\text{cut}}^{\text{PW}}=80$ Ry to better access the small differences in energy associated with φ_{N}. Closely related to the observation of a shallow energy hypersurface is a

notable dependency of the structural results (optimal lattice constant and internal coordinates) on the plane-wave cutoff chosen. We found that only the relatively large cutoff $E_{\mathrm{cut}}^{\mathrm{PW}} = 80$ Ry is sufficient for convergence of lattice properties. For example: the optimum lattice constant for SiC_2N_4 structures was 2% smaller using $E_{\mathrm{cut}}^{\mathrm{PW}} = 40$ Ry; the rotation angle ψ_{N} in Si_2CN_4 structures decreased by 5° on increasing the basis. We noticed that the bond angle φ_{N} in all structures converges when $E_{\mathrm{cut}}^{\mathrm{PW}}$ gets high enough. Thus, a ''correct'' evaluation of the shallow energy hypersurface for these particular structures needs quite a big expansion of the electronic wave function into plane waves.

For the final relaxations we also used a finer grid to generate **k** points for the SiC_2N_4 structures. The [4,4,4] grid resulted in four special **k** points for $Pn\bar{3}m$ and six **k** points for $P\bar{4}n2$. A [4,4,2] grid was used for the $P4_322$ structure of SiC_2N_4 leading to three **k** points. These settings were also used to calculate the energy-volume diagrams which were fitted using the Murnaghan equation of state to calculate ground-state properties.[62] For both structures of Si_2CN_4 we also used the two **k**-point set for relaxations with the larger basis. Finer grids for all structures were employed (without relaxation) to access the level of convergence for our **k**-point sampling.

For the various errors in our scheme (optimization procedure, **k**-point sampling and $E_{\mathrm{cut}}^{\mathrm{PW}}$), we estimate that the level of precision we achieved with the computational method guarantees that energy differences between structures of identical stoichiometry (identical local bonding), thus within SiC_2N_4 and within Si_2CN_4, are correct within 1–2 meV per atom (1σ), thus ≈ 0.01 eV per formula unit (≈ 1 kJ/mol).

Shear constants were computed assuming no symmetry for the structures. For SiC_2N_4 in $P\bar{4}n2$, we used a [222] grid (four **k** points) to assure that c_{44} is positive. The same grid was used (and needed) for the calculation of the shear constants (c_{44}, c_{55}, c_{66}) for the Si_2CN_4-structures ($Aba2$ and $Cmc2_1$). Finally, the band structures we present (for $P\bar{4}n2$-SiC_2N_4 and $Aba2$-Si_2CN_4) were calculated using the optimized geometries and $E_{\mathrm{cut}}^{\mathrm{PW}} = 80$ Ry.

[1] *Handbook of Ternary Alloy Phase Diagrams*, edited by P. Villars, A. Prince, and H. Okamoto (ASM International, Ohio, 1995), Vol. 6.

[2] *Phase Diagrams in Advanced Ceramics*, edited by A. Alper (Academic, London, 1995).

[3] *Silicon Carbide Electronic Materials and Devices* [MRS Bull. **22** (1997)].

[4] *SiC Materials and Devices*, edited by Y. S. Park, Semiconductors and Semimetals Vol. 52, edited by R. K. Willardson and R. Weber (Academic Press, San Diego, 1998).

[5] *Fundamental Questions and Applications of SiC*, edited by W. J. Choyke, H. Matsunami, and G. Pensl, special issue of Physica Status Solidi [Phys. Status Solidi A **162** (1997); Phys. Status Solidi B **202** (1997)].

[6] K. Komeya and M. Matsui, *High Temperature Engineering Ceramics*, in *Structure and Properties of Ceramics*, edited by M. Swain, in Materials Science and Technology, edited by R. W. Cahn, P. Haasen, and E. J. Kramer, Vol. 11 (VCH, New York, 1996).

[7] K. Niihara, J. Ceram. Soc. Jpn. **99**, 974 (1991).

[8] F. Wakai, Y. Kodama, S. Sakaguchi, N. Murayama, K. Izaki, and K. Niihara, Nature (London) **344**, 421 (1990).

[9] R. Riedel, H.-J. Kleebe, H. Schönfelder, and F. Aldinger, Nature (London) **374**, 526 (1995).

[10] A. Liu and M. L. Cohen, Science **245**, 841 (1989).

[11] C. Niu, Y. Z. Lu, and C. M. Lieber, Science **261**, 334 (1993).

[12] J. V. Badding, Adv. Mater. **9**, 877 (1997).

[13] H. Rucker, M. Methfessel, E. Bugiel, and H. Osten, Phys. Rev. Lett. **72**, 3578 (1994).

[14] J. Kouvetakis, D. C. Nesting, M. O'Keeffe, and D. J. Smith, Chem. Mater. **10**, 1396 (1998).

[15] J. Kouvetakis, D. Shandrasekhar, and D. J. Smith, Appl. Phys. Lett. **72**, 930 (1998).

[16] R. Riedel, in *Processing of Ceramics*, edited by R. J. Brook, in Materials Science and Technology, edited by R. W. Cahn, P. Haasen, and E. J. Kramer, Vol. 17B (VCH, New York, 1996).

[17] S. Schempp, J. Dürr, P. Lamparter, J. Bill, and F. Aldinger, Z. Naturforsch., A: Phys. Sci. **53**, 127 (1998).

[18] R. Riedel, A. Greiner, G. Miehe, W. Dressler, H. Fuess, J. Bill, and F. Aldinger, Angew. Chem. Int. Ed. Engl. **36**, 603 (1997).

[19] R. W. G. Wyckoff, Am. J. Sci. **209**, 448 (1925).

[20] I. Idrestedt and C. Brosset, Acta Chem. Scand. **18**, 1879 (1964).

[21] X. Sjoeberg *et al.*, Acta Crystallogr., Sect. C: Cryst. Struct. Commun. **47**, 2438 (1991).

[22] H.-D. Schädler, L. Jäger, and I. Senf, Z. Anorg. Allg. Chem. **619**, 1115 (1993).

[23] A. Greiner, Ph.D. thesis, University of Technology Darmstadt, 1997.

[24] R. Franke, St. Bender, P. Kroll, A. Greiner, and R. Riedel, J. Electron Spectrosc. Relat. Phenom. **96**, 253 (1998).

[25] R. Riedel, E. Kroke, A. Greiner, A. O. Gabriel, L. M. Ruwisch, J. Nicolich, and P. Kroll, Chem. Mater. **10**, 2964 (1998).

[26] A. Obermeyer, A. Kienzle, J. Weidlein, R. Riedel, and A. Simon, Z. Anorg. Allg. Chem. **620**, 1357 (1994).

[27] M. Jansen and H. Jüngermann, Z. Kristallogr. **209**, 779 (1994).

[28] A. Hammel, H. V. Volden, A. Haaland, J. Weidlein, and R. Reischmann, J. Organomet. Chem. **408**, 35 (1991).

[29] C. Glidewell and A. G. Robiette, Chem. Phys. Lett. **28**, 290 (1974).

[30] T. Pasinski, T. Veszprémi, and M. Fehér, J. Mol. Struct.: THEOCHEM **331**, 289 (1995).

[31] M. T. Nguyen, N. V. Riggs, L. Radom, M. Winnewisser, B. P. Winnewisser, and M. Birk, Chem. Phys. **122**, 305 (1988).

[32] S. R. Batten and R. Robson, Angew. Chem. Int. Ed. Engl. **37**, 1460 (1998).

[33] W. A. Dollase, Z. Kristallogr. **121**, 369 (1965).

[34] A. F. Wright and A. J. Leadbetter, Philos. Mag. **31**, 1391 (1975).

[35] M. O'Keeffe and B. G. Hyde, Acta Crystallogr., Sect. B: Struct. Crystallogr. Cryst. Chem. **32**, 2923 (1976).

[36] P. Hohenberg and W. Kohn, Phys. Rev. A **136**, 864 (1964).

[37] W. Kohn and L. J. Sham, Phys. Rev. A **140**, 1133 (1965).

[38] R. M. Dreizler and E. K. U. Gross, *Density Functional Theory* (Springer-Verlag, Berlin, 1990).

[39] R. G. Parr and W. Wang, *Density-Functional Theory of Atoms and Molecules* (Oxford University Press, New York, 1989).
[40] ADF 2.3.0, Theoretical Chemistry, Vrije Universiteit, Amsterdam (1997).
[41] G. te Velde and E. J. Baerends, J. Comput. Phys. **99**, 84 (1992).
[42] C. Fonseca Guerra, O. Visser, J. G. Snijders, G. te Velde, and E. J. Baerends, in *Methods and Techniques for Computational Chemistry*, edited by E. Clementi and G. Corongiu (STEF, Cagliari, Italy, 1995), pp. 305–395.
[43] J. G. Snijders, E. J. Baerends, and P. Vernoojis, At. Data Nucl. Data Tables **26**, 483 (1982).
[44] E. J. Baerends, D. E. Ellis, and P. Ros, Chem. Phys. **2**, 41 (1973).
[45] S. H. Vosko, L. Wilk, and M. Nusair, Can. J. Phys. **58**, 1200 (1980).
[46] A. D. Becke, J. Chem. Phys. **84**, 4524 (1986).
[47] A. D. Becke, Phys. Rev. A **38**, 3098 (1988).
[48] J. P. Perdew, Phys. Rev. B **33**, 8822 (1986); **34**, 7406(E) (1986).
[49] D. M. Ceperley and B. J. Alder, Phys. Rev. Lett. **45**, 566 (1980).
[50] J. P. Perdew and A. Zunger, Phys. Rev. B **23**, 5048 (1981).
[51] L. Kleinman and D. M. Bylander, Phys. Rev. Lett. **48**, 1425 (1982).
[52] D. R. Hamann, Phys. Rev. B **40**, 2980 (1989).
[53] N. Troullier and J. L. Martins, Phys. Rev. B **43**, 1993 (1991).
[54] M. Fuchs and M. Scheffler, Comput. Phys. Commun. **119**, 67 (1999).
[55] H. J. Monkhorst, J. D. Pack, Phys. Rev. B **13**, 5188 (1976).
[56] R. P. Feynman, Phys. Rev. **56**, 340 (1939).
[57] M. Bockstedte, A. Kley, J. Neugebauer, and M. Scheffler, Comput. Phys. Commun. **107**, 187 (1997).
[58] This we have consistently found for many carbodiimides. P. Kroll and R. Hoffmann (unpublished).
[59] G. M. Sheldrick and R. Taylor, J. Organomet. Chem. **101**, 19 (1975).
[60] A. Kienzle, A. Obermeyer, R. Riedel, F. Aldinger, and A. Simon, Chem. Ber. **126**, 2569 (1993).
[61] Let us note here two things: First, we calculated the distance $d_{\mathrm{Si\text{-}N}}$ for the molecule $N(SiH_3)_3$ to be 1.758 Å. Thus, the bond length in the silyl-carbodiimides is shorter. Second, we get a (greater) dimunition of $d_{\mathrm{Si\text{-}N}}$ for the molecular model in case of the tetramer, $Si(NCNSiH_3)_4$. The bond length (assuming C_2 symmetry) then is 1.69 Å.
[62] F. D. Murnaghan, Proc. Natl. Acad. Sci. USA **30**, 244 (1944).
[63] A. Y. Liu and M. L. Cohen, Phys. Rev. B **41**, 10 727 (1990).
[64] C. H. Park, B.-H. Cheong, K.-H. Lee, and K. J. Chang, Phys. Rev. B **49**, 4485 (1994).
[65] F. Liu, S. H. Garofalini, R. D. King-Smith, and D. Vanderbilt, Phys. Rev. B **49**, 12 528 (1994).
[66] T. A. Mary, J. S. O. Evans, T. Vogt, and A. W. Sleight, Science **272**, 90 (1996).
[67] N. Khosrovani and A. W. Sleight, J. Solid State Chem. **121**, 2 (1996).
[68] For this we took the internal coordinates of the $Pn\bar{3}m$ structure and distorted them into $P\bar{4}n2$ (dropping any threefold axes, as well as the inversion center) allowing the atoms to relax. In the asymmetric unit, the movement of C is along the (normalized) vector $(-0.71,+0.71,0)$, that of N along $(-0.78,0.62,0.05)$.
[69] J. F. Nye, *Physical Properties of Crystals* (Oxford Science, Clarendon, Oxford, 1985).
[70] For the alternative structure of Si_2CN_4 with space-group symmetry $Cmc2_1$ we used the nonstandard setting $Ccm2_1$ to facilitate direct comparison to the $Aba2$ structure. Alternatively, we could also have chosen the nontandard setting $Bba2$ for the latter one.
[71] W. L. Jorgensen and L. Salem, *The Organic Chemists Book of Orbitals* (Academic, New York, 1973), p. 128f.
[72] We did the rationalizing with the help of extended Hückel calculations, for which the band structure looks very similar.
[73] B. G. Hyde and S. Andersson, *Inorganic Crystal Structures* (Wiley, New York, 1989), p. 59.
[74] C. T. Prewitt and R. D. Shannon, Acta Crystallogr., Sect. B: Struct. Crystallogr. Cryst. Chem. **B24**, 869 (1968).